Journal of Great Lakes Research 48 (2022) 876–889

Contents lists available at ScienceDirect

Journal of Great Lakes Research

journal homepage: www.elsevier.com/locate/ijglr

Desiccation of the Transboundary Hamun Lakes between Iran and Afghanistan in Response to Hydro-climatic Droughts and Anthropogenic Activities

Mahdi Akbari [a,*], Ali Mirchi [b], Amin Roozbahani [c], Abror Gafurov [d], Bjørn Kløve [a], Ali Torabi Haghighi [a]

[a] Water, Energy and Environmental Engineering Research Unit, Faculty of Technology, University of Oulu, Finland
[b] Department of Biosystems and Agricultural Engineering, Oklahoma State University, Stillwater, United States
[c] Nimab-tose Consulting Engineering Company, Tehran, Iran
[d] GFZ German Research Centre for Geosciences, Section 5.4 Hydrology, Potsdam, Germany

ARTICLE INFO

Article history:
Received 5 July 2021
Accepted 5 May 2022
Available online 14 May 2022
Communicated by Somayeh Sima

Keywords:
Standardized Precipitation Index (SPI)
Standardized Discharge Index (SDI)
Normalized Difference Spectral Indices (NDSIs)
Water management
Lake desiccation
Aral-Sea syndrome

ABSTRACT

This paper investigates the hydro-climatic reasons behind the desiccation of the Hamun Lakes in the Iran-Afghanistan border. We analyzed changes in the flow of the Hirmand River (90 percent of the total inflow to the lakes) at the international border, and precipitation over this river's sub-basin during 1960–2016 by calculating standardized indices for precipitation (SPI) and discharge (SDI). We applied Normalized Difference Spectral Indices using satellite images from 1987 to 2021 to observe monthly areal change of the lakes. The results show that the major cause of desiccation is upstream water regulation which severely reduced the Hirmand River inflow delivery to the lakes. Constructed reservoirs near the lakes by Iran in 2008, compounded the effect of Afghanistan water regulation to aggravate the situation. There is a discernible shift in the relation between the Hirmand River flow at the border and upstream precipitation before and after 2004. In 1960–2003, high Hirmand River inflows were expected due to high precipitation, while the flow declined after 2004 despite large amounts of upstream precipitation. Although a long period of drought from 1998 to 2004 decreased the lakes' area, the lake system is primarily falling victim to anthropogenic flow reduction recently. Increased regulation of flows and use of water for irrigation in Afghanistan and Iran underscores the necessity of bilateral dialogues between the two countries to consider environmental flow for the lakes. The lakes' shrinkage places socio-economic stress on an already-vulnerable region with public health implications as the exposed lake beds turn into major sources of dust storms.

Introduction

The Hamun Lakes are the largest (>8000 km^2) fresh body of water in the Iran plateau and have been desiccated after 2005 (Pekel et al., 2016). Climatic variation is an important driver of the change of water-land at large scales (Akbari et al., 2020; Ehsani et al., 2020; Haghighi and Kløve, 2015; Milly and Dunne, 2016; Rahimi et al., 2020). However, there is growing concern that human activities are a substantial, sometimes dominant reason for decline of water bodies, triggering a host of environmental and economic consequences (AghaKouchak et al., 2015; Chaudhari et al., 2018; Torabi Haghighi et al., 2020; Khazaei et al., 2019; Abou Zaki et al., 2020). For example, the shrinkage of water bodies due to anthropogenic effects (e.g. agricultural activities), i.e., so-called Aral-Sea desiccation syndrome (AghaKouchak et al., 2015), have been documented in Central Asia (Micklin, 1988) and northwestern Iran (Akbari et al., 2019; Alborzi et al., 2018).

The Hamun Lakes are crucial for the economy and environment of the surrounding area (Rashki et al., 2012). The main rivers that sustain the lakes originate in Afghanistan. Hirmand (or Helmand) River, the most important river feeding the lake system and a crucial water source for Afghan and Iranian farmers (Ahlers et al., 2014), is shared based on a bilateral treaty in 1973 (Helmand Commission, 1973). The 1973 agreement guarantees to supply Iran with an average 22 m^3/s plus 4 m^3/s (for "goodwill and brotherly relations"), providing a basis for monthly allocation of the Hirmand River flow to Iran. Thus, Iran's annual share of Hirmand River flow is about 0.82 km^3 (Fig. 1f). Monthly flow deliveries are based on

* Corresponding author.
E-mail address: mahdi.akbari@oulu.fi (M. Akbari).

https://doi.org/10.1016/j.jglr.2022.05.004

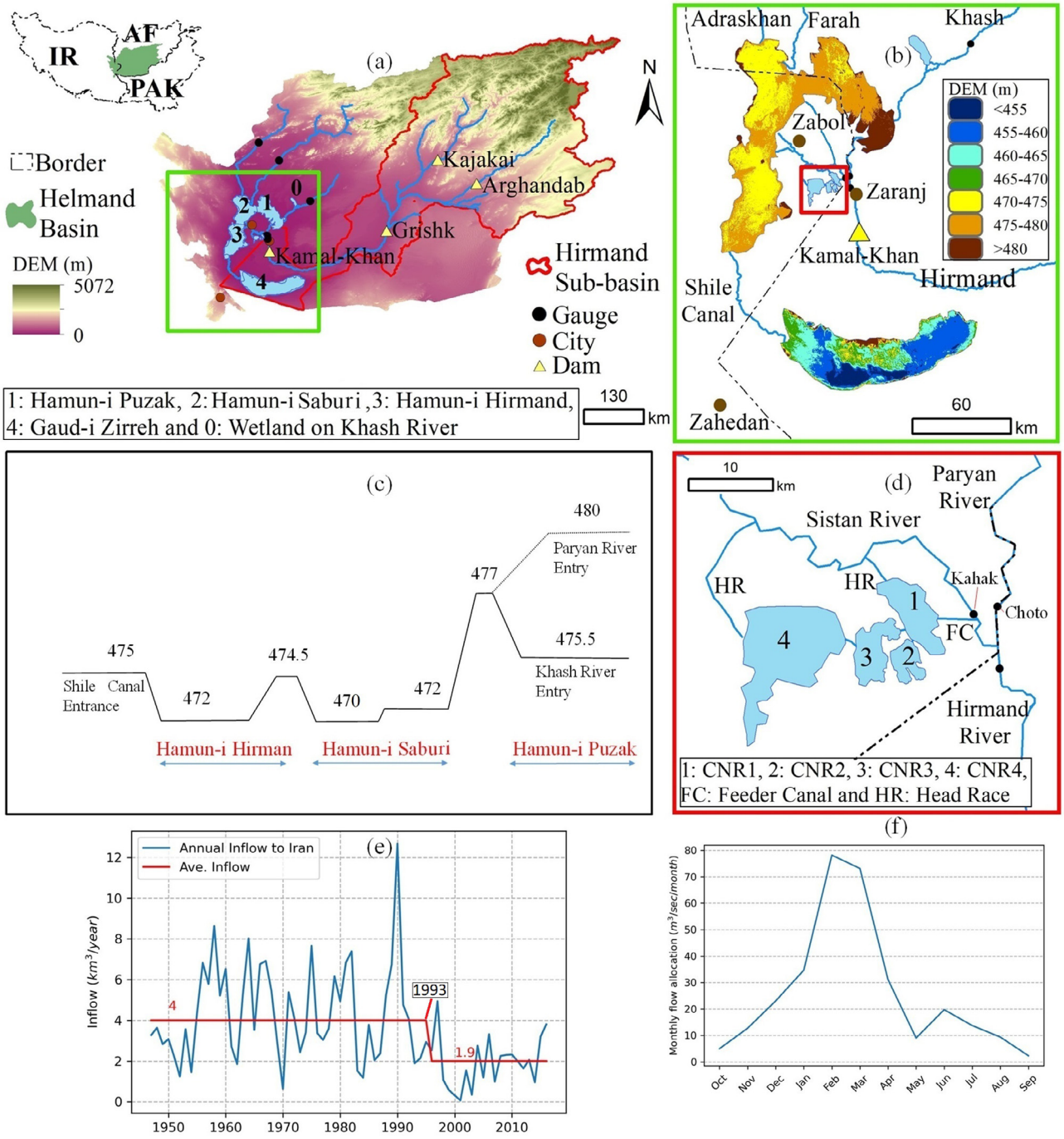

Fig. 1. Study area: a) Helmand Basin, Hirmand River sub-basin and Hamun Lakes with the location of dams, inflow gauges and cities, b) DEM of Hamun Lakes and close water bodies to Hamun Lakes, c) transverse profile of Hamun Lakes (HIWRI, 2017), d) Hirmand, Sistan and Paryan Rivers next to border between Iran and Afghanistan, CNRs, Head Races and Feeder Canal, e) annual inflow of Hirmand River in the location of Iran-Afghanistan border from 1960 to 2016 (average flow shift in 1993) and f) guaranteed monthly Hirmand River flow to reach Iran based on the bilateral treaty between Iran and Afghanistan in 1973 (ref: MoE, 2013).

"normal water years" (Article II), which is defined as a year with total flows upstream of Kajaki Dam being more than 5.661 km^3 between 1 October and the following 30 September (Article I). Therefore, this treaty is flexible in dry years, i.e., water deliveries are adjusted proportionally to deviations from predefined normal years (Article IV). Also, Afghanistan must supply water of a quality that can be treated, if necessary, for irrigation and domestic uses (Art. VI). The 1973 treaty does not address the environmental water right of the Hamun Lakes; thus, Iran utilizes 0.82 km^3 of water considered in the treaty for potable and agricultural uses. DOE, estimated that annually 7.67 km^3 environmental flow is needed for ecological restoration of the lakes (Iran Department of Environment (DOE) (2014)). Other studies (Amini et al., 2021; Thomas and Varzi, 2015), confirmed the inadequacies of the 1973 treaty for sustainable transboundary water resources management in which the right of the lakes to environmental flow is considered. Recent agricultural development and water resources management in the region are giving rise to classic

upstream-downstream water tensions that adversely affect the socio-economically vulnerable residents in the border region, including the Sistan and Baluchistan provinces of Iran (Ahlers et al., 2014).

The Hamun Lakes are a major dust source in southwest Asia (Goudie and Middleton, 2006) due to strong winds (known as "120-day wind") in the region (Hossenzadeh, 1997). The communities around the lakes are affected by post-desiccation dust storms (Rashki et al., 2012). Furthermore, the sand and dust storms affect the whole Sistan region in Iran, southwest Afghanistan, and Pakistan (Alam et al., 2011; Goudie and Middleton, 2000; Rashki et al., 2012). Zaranj City (Fig. 1-b) is the largest population center (~160,000 people) in Afghanistan close to the lakes (Afganistan Ministry of Urban Development Affairs, 2015). The population in urban areas is larger on the Iranian side where Zahedan (~670,000) and Zabol (~165,000) are located (Statistical Center of Iran, 2016). In 2012 Zabol had the most polluted air in the world. In this year, the concentration of mean annual particulate matter with 10 and 2.5 μm or less in diameter (PM_{10} and $PM_{2.5}$) in Zabol reached 527 and 217 $\mu g/m^3$, respectively (WHO, 2016), far exceeding WHO's safe concentration thresholds for PM_{10} (20 $\mu g/m^3$) and $PM_{2.5}$ (10 $\mu g/m^3$). Consequently, respiratory diseases are a common public health hazard in Zabol with medical costs exceeding USD 73.5 million during 1999–2004 (Miri et al., 2007).

As mounting concerns about the drying of the Hamun Lakes give rise to potential water conflicts in this transboundary basin (Dehgan et al., 2014; Mianabadi et al., 2021), it is necessary to evaluate whether the shrinkage is governed by climatic conditions or if the problem has emerged as a result of anthropogenic water regulation. This understanding is an important precursor for effective plans to protect the socio-ecological system based on binational cooperation between Iran and Afghanistan. To this end, we investigate the climatic and hydrological drivers of the lakes' desiccation alongside a shift in water management paradigm that has marginalized environmental flows. Our analysis covers water resources management on both sides of the border, namely upstream dams in Afghanistan, as well as water regulation of the Hirmand River in Iran enabled by constructing reservoirs in the Sistan region. We study hydrological and meteorological droughts in the Hirmand River sub-basin from 1960 to 2016 to characterize the Hirmand River flow alteration at the international border. Notwithstanding the hydro-political complexity of the transboundary region, our hydro-climatological investigation of the connected lakes provides useful insights into the mechanism of desiccation and potential reasons behind the decline of the connected lakes.

Materials and methods

Study area

Hamun Lakes are in the Iran-Afghanistan border zone in the Sistan region (Fig. 1-a) within the transboundary Helmand Basin. The lake system is a Ramsar site (The Convention on Wetlands, 1975). Helmand Basin (area: ~350,000 km^2) is the largest basin in Afghanistan, covering 43% of the country. Most of this transboundary basin (~80%) is in Afghanistan, less than 5% in Pakistan and the rest in Iran (Fig. 1a). Hirmand River sub-basin is a part of the Helmand Basin as shown in Fig. 1a. As the terminal point of an endorheic basin, the Hamun Lake system is primarily fed by rivers that originate in the Hindu Kush mountain range. Other major tributaries besides the Hirmand (or Helmand) River (mean annual flow: ~ 6 km^3) include Farah, Khash, Khospas and Adraskan (or Harut) (Fig. 1a). Total inflow from Farah, Khash, Khospas, Adraskan and other minor tributaries is 0.54 km^3 (Iran Department of Environment (DOE), 2014). Thus, over 90 percent of total inflow to the lakes is provided by the Hirmand River. Two of the largest dams in Afghanistan, namely Kajaki (capacity 2.5 km^3) and Arghandab (or Dahla, capacity 0.5 km^3), were built in this basin in 1952 (Lehner et al., 2011). Based on data from 1960 to 1980, the maximum monthly inflow to these dams occurred in April, averaging about 1.5 and 0.6 km^3, respectively (Williams-Sether, 2008). Also, the Kamal-Khan Dam with current capacity equal to 0.05 km^3 is the largest hydraulic structure on the Hirmand River after the Kajaki Dam (Fig. 1a). Construction of the Kamal-Khan Dam began in 1996, but it was halted due to the civil war in Afghanistan. The project recommenced in 2011 and phase II was completed in 2015. Work on phase III began in 2017, and the dam went into operation in 2021. The objective has been to provide water for irrigation of agricultural land in Afghanistan, flood protection, drinking water and generation of 9 MW of electricity.

According to the Köppen-Geiger climate classification (Kottek et al., 2006), the Helmand Basin's climate varies from highlands to downstream areas, ranging from snow climate with dry summers (Ds) in the Hindu Kush mountain range to warm temperate climate with dry summer (Cs) in the foothills of the Hindu Kush mountains and steppe climate (BS) and desert climate (BW) downstream of Kajaki and Arghandab Dams (Electronic Supplemenatry Material (ESM) Appendix A, Fig. S1a). Based on the Global Precipitation Climatology Centre (GPCC) dataset (Schneider et al., 2011), the basin's annual precipitation varies from more than 1200 mm in the Hindu Kush highlands to less than 60 mm in the lowlands near the Hamun Lakes (see ESM Appendix B). Also, in the Sistan region, "120-Day winds" are frequent and intensive, especially during the summer (Goudie and Middleton, 2000), and their speed reaches over 100 km/s (Meteorological Department of Sistan and Baluchestan, 2020).

The Hamun Lakes consist of three connected Lakes above Shile Canal (Fig. 1b), namely Hamun-i Puzak ($\max area = 1500$ km^2), Hamun-i Saburi ($\max area = 1500$ km^2) and Hamun-i Hirmand ($\max area = 2000$ km^2), and a deeper terminal lake named Gaud-i Zirreh ($max\,area = 3000$ km^2) (Fig. 1a). Hamun-i Puzak with an elevation of 480 m (m) above mean sea level (AMSL) at the outlet of the Paryan River (Fig. 1c) is the first lake in this cascading lake system. The lowest bed elevation at Hamun-i Puzak is 475.5 m AMSL, and excess flow after filling this lake spills into Hamun-i Saburi at 477 m AMSL, which discharges into the downstream Hamun-i Hirmand at 474.5 m AMSL (Fig. 1c). Finally, the last lake is Gaud-i Zirreh, which is fed by Shile Canal in the south of Hamun-i Hirmand (Fig. 1b). Mean depth of the first three lakes (Hamun-i Puzak, Hamun-i Saburi and Hamun-i Hirmand) is one meter (ModaresiRad et al., 2022), while Gaud-i Zirreh is the deepest lake with a mean depth of 10 m. Mean annual flow for Shile Canal (inflow to Gaud-i Zirreh) at Pol-Shile station is about 3 km^3 (1990–1998), which decreased to almost zero after 1999 (Hamoon International Wetland Research Institute of Zabol University (HIWRI) (2017)).

Hirmand River bifurcates into two rivers after entering Iran, the Sistan and Paryan Rivers (Fig. 1d). Paryan River flows to Hamun-i Puzak, and Sistan River finally ends in Hamun-i Saburi and Hamun-i Hirmand (Fig. 1b). Based on long-term flow data (gauges shown in Fig. 1d), 47% of the total inflow of the Hirmand River is observed in Choto gauge on the Paryan River while the rest is recorded by Kahak gauge on the Sistan River (MoE (2014)). Some parts of the Sistan River flow were diverted by Kahak diversion dam (Fig. 1d) to four reservoirs named Chah Nimeh Reservoirs (CNR1 through 4) by the Feeder Canal (shown as FC in Fig. 1d with capacity = 600 m^3/sec). CNR1 (Cap: 0.220 km^3), CNR2 (Cap: 0.090 km^3), and CNR3 (0.320 km^3) were constructed in 1983. The last and largest reservoir, i.e. CNR4 (Cap: 0.810 km^3) was commissioned in 2008 but initial filling began sooner (Absaran Consulting

Company, 2015). The main purposes of CNRs in Iran are to meet agricultural (0.4 km^3/yr), domestic (0.11 km^3/yr), and industrial (0.03 km^3/yr) demands of the Sistan region based on the current status of the basin, totaling 0.54 km^3/yr (MoE (2014)). CNRs are connected, each spilling to the next at 480 m AMSL. Feeder Canal discharges into CNR1, and then into CNR2 until all CNRs are sequentially filled. When all CNRs are full, the overflow is directed to the Sistan River from the north of CNR1 and west of CNR4 by two canals known as Head Race (HR shown in Fig. 1d). Both HRs have been equipped with floodgate to regulate outflow. Near CNRs pan evaporation is reported to be 4,836 mm/yr and annual potential evaporation from water surface in the Sistan region is estimated to be 2585 mm (Iran Department of Environment (DOE), 2014). Also, the annual volume of actual evaporation from the CNRs water surface is 0.306 km^3 (MoE (2014)).

Data

The spatiotemporal scope of the study was determined based on data availability and predominant inflow into the lakes. We limited our investigation to Hirmand River sub-basin (Fig. 1a) for 1960–2016 because over 90 percent of the total flow to the lakes is provided by this river. The annual flow data (Fig. 1e) from 1960 to 2016 for Choto and Kahak gauges on Sistan and Paryan Rivers next to the border on the Iranian side (Fig. 1d) were obtained from Iran Ministry of Energy (Iran Ministry of Enegry (MoE) (2013)). Also, the USGS data-base (Williams-Sether, 2008) provides flow data for period 1955–1980 at gauges located in Afghanistan (Fig. S1).

We calculated annual precipitation and inflow based on the defined water year in the 1973 treaty (i.e., from the first of October to the end of following year September). Available rain gauge data in the study area in Afghanistan and Iran do not have good spatial and temporal coverage. Thus, we used widely-applied satellite-based rainfall products, namely GPCC (Schneider et al., 2011), PERSIANN-CDR (Ashouri et al., 2015) and TRMM-3B43 (Huffman et al., 2007). All of these products show high amount of precipitation in the region in the 2010–2016 period (more detail in ESM Appendix B). We utilized different sources of precipitation products to ensure that the increasing trend of precipitation is recorded by various data sources. A comprehensive evaluation of currently available precipitation datasets over Iran at monthly (44 datasets) and daily (34 datasets) time scales (Saemian et al., 2021) as well as European Centre for Medium-Range Weather Forecasts Reanalysis (ERA) precipitation product (Ghajarnia et al., 2021) have shown that the GPCC overall matches the rain gauges network records better than other products over eastern basins of Iran. Therefore, we used the GPCC to estimate precipitation over the Hirmand River sub-basin from 1960 to 2016. Also, satellite images from MODIS and Landsat were used to monitor water bodies area change. Digital elevation model (DEM) data are from ALOS World 3D-30 m (AW3D30) (Tadono et al., 2016).

Methodology

Water body detection

The Normalized Difference Spectral Indices (NDSIs) are commonly used for surface water detection (Boschetti et al., 2014). Among different NDSIs, those using visible bands (such as red, green, etc.), near-infrared band and short wave near infrared band have been shown to outperform others (Boschetti et al., 2014). The Normalized Difference Vegetation Index (NDVI) and the Normalized Difference Water Index (NDWI) are two examples of this class of NDSIs, which facilitate water detection (Chipman and Lillesand, 2007; Ouma and Tateishi, 2006; Pekel et al., 2016; Rokni et al., 2014; Rouse, 1973; Abou Zaki et al., 2018). Both indices are based on normalized difference of bands in the electromagnetic spectrum and vary between −1.0 to 1.0:

$$NDWI = (NIR - SWIR)/(NIR + SWIR) \quad (1)$$

$$NDVI = (NIR - Red)/(NIR + Red) \quad (2)$$

where NIR, RED and SWIR are reflections in the near-infrared, red visible and short wave near infrared.

Positive NDWI and negative NDVI values represent water. Specific thresholds are needed to determine water surfaces from other land cover types. We have access to multispectral remotely sensed products from different satellites, such as Sentinel, Landsat, and MODIS. We utilized MODIS images available after year 2001 because daily temporal resolution of this product helps resolve the common cloud cover issue by providing more images in each month. Furthermore, we used Landsat images available for the study area from 1987 to 2001 to expand our temporal coverage. We used MODSI NDWI and Landsat NDVI products due to their good quality (i.e., less noise) in the study region to determine the monthly variation of the water bodies' area. Using Google Earth Engine Java Script API (Gorelick et al., 2017) (the source code is available at the end of manuscript-Data availability section), appropriate thresholds for NDVI and NDWI are suggested as 0.03–0.04 and 0.1–0.17 respectively. All Google Earth Engine Java Script API source codes are available for monthly and annual water surface detection from 1987 to present (https://code.earthengine.google.com/3da29654956ce83cdd8db500770b7caf?noload = true%20) and for precipitation calculation (https://code.earthengine.google.com/5e14fcbbff9e0828b698340f58eb9628?noload = true)

Hamun Lakes rate of desiccation

We quantified the monthly rate of desiccation (i.e., d(area)/d(time)) for Hamun Lakes when they receive no inflow. The monthly flow of Hirmand River at the border was zero from March 1999 to August 2002, providing a suitable timeframe for the analysis. We used the monthly area of all Hamun Lakes from Landsat and MODIS satellites during this period to estimate how fast Hamun Lakes desiccate after the inflow is cut. Quantifying the rates of desiccation can show how fast each lake desiccates. This rate is affected by the depth of each water body because evaporation rate is faster in shallower lakes.

Sensitivity of the Hamun lakes area to monthly inflow

The relationship between Hirmand inflow and the lakes' area was investigated based on monthly area and inflow of Hirmand River to Iran from Jan. 1987 to Aug. 2013, i.e., the period with available monthly flow data. We defined three classes of monthly inflow: 1) inflow less than 0.5 km^3 (275 cases), 2) inflow between 0.5 and 1 km^3 (30 cases) and 3) inflow more than 1 km^3 (15 cases). We chose 0.5 km^3 as a threshold of runoff classes because this is approximately equal to the active capacity of CNR4. This approach allowed an investigation of how the new water regulation capacity of CNR4 can affect the area of the lakes.

Drought indices (SPI and SDI)

Using annual (Oct. to Sep.) precipitation and runoff, we calculated Standardized Precipitation Index (SPI) and Standardized Discharge Index (SDI). To analyze the temporal hydro-climatological status of the Hirmand River sub-basin, the trend, the variation, and the average value of rainfall and discharge were calculated. Temporal climate variability was characterized using SPI, which is designed to evaluate metrological drought (McKee, 1995) and has been widely used for evaluating climate variability (Hao et al., 2014; Irannezhad et al., 2015). SPI requires fitting a probability density function (McKee, 1995; Thom, 1966) to the frequency

distribution of precipitation at a given station for a particular timescale (e.g. 3 months and 6 months). In this study, annual SPI was estimated as (Farahmand and AghaKouchak, 2015):

$$SPI = \varnothing^{-1}(p) \quad (3)$$

where $\varnothing$ is the standardized normal distribution function and p is the corresponding empirical probability when the precipitation in Hirmand River sub-basin is sorted in ascending order. Based on SPI, climate conditions can be divided into eight categories as classified in Table 1.

SDI is calculated using the same approach as SPI but using the recorded annual river flow of Hirmand River at the Iran-Afghanistan border instead of precipitation. SPI and SDI are used to describe various drought categories. Over time, increased water consumption typically occurs in the upstream part of many basins. Increasing upstream water withdrawal or land-use change which can significantly alter river flow, and subsequently downstream water delivery. Comparison between SPI and SDI can reveal how the association between upstream precipitation and downstream flow is impacted by climatic or anthropogenic drivers in the long term (Shukla and Wood, 2008). Also, we compared results of SPI with Standardized Precipitation Evapotranspiration Index (SPEI) to consider the effect of evapotranspiration. It was found that SPI and SPEI are consistent in terms of categorizing years based on drought condition (more detail in ESM Appendix D).

Limitations and data uncertainty

Lack of information and data is a major barrier for Afghanistan's engagement with riparian neighbors on transboundary issues. Since 1979, no hydrologic data has been published publicly in this country (Ahlers et al. 2014; Williams-Sether 2008) thereby increasing uncertainties. For example, an accurate estimation of the magnitude of discharge into the Hamun Lakes is not possible (MoE (2015)), primarily due to the lack of river flow data in Afghanistan, especially on the northern tributaries. Using the main river flow data is recommended in the literature to characterize the hydrologic conditions to the extent possible despite lack of data on other feeding tributaries (Akbari et al., 2020; Chen et al., 2017). We used flow data at the border available from Iran. However, the amount of water diversions from the Hirmand River between the border and the water bodies is not available. Additionally, due to lack of water level data for the lakes, the best thresholds to detect water by NDVI and NDWI were selected by comparing different thresholds' results with Pekel et al. (2016) study (more detail in ESM Appendix E). Also, based the evaporation pan records in the Zabol synoptic station, the trend of monthly evaporation throughout the year is zero or negative in the majority of months during 1993–2017 period (ESM Appendix D Fig. S7). While we did not explicitly consider the effect of evaporation, the trend suggests that this climatic parameter does not aggravate the situation for the lakes.

Table 1
Different categories of climatological conditions based on the SPI and SDI values.

Category	Range of drought indices (SPI/SDI)
Extremely wet	More than 2.00*
Very wet	1.50–1.99*
Moderately wet	1.00–1.49*
Mildly wet	0.00–0.99*
Mild drought	–0.99 to 0.00*, **
Moderate drought	–1.49 to – 1.00*, **
Severe drought	–2.00 to – 1.50*, **
Extreme drought	<–2.00*, **

* Lloyd-Hughes and Saunders (2002).
** McKee et al. (1993).

Results

Areal change of the lakes and CNRs in the Sistan region

The monthly area of CNRs (Fig. 2e–h) shows that these reservoirs did not experience complete desiccation for all operating years except at the beginning of the 2000s due to extremely dry conditions (Table 1). However, monthly area variation in the Hamun Lakes is high. Sometimes the area approaches zero, i.e., complete desiccation (boxplot in Fig. 2a–d). The CNRs exhibited low variation in monthly average area in all years of operation (boxplots in Fig. 2e–h). Therefore, coefficients of variation for monthly areas are 8.4%, 8.8%, 3.8% and 26.4% for CNR1 to CNR4 respectively.

Monthly area of the Hamun Lakes (Fig. 2a–d) starts to decrease after April-May when flow diminishes in the region (Fig. 5d). However, Gaud-i Zirreh has completely desiccated (Fig. 2d) because inflow to Shile Canal has approached zero since 1999. The monthly areal change of this water body has different pattern than the other lakes (boxplot of Fig. 2d). CNR1, CNR2 and CNR3 also reached maximum area in April-May (boxplots in Fig. 2e–g) when Hirmand River deliveries to Iran increased (Fig. 5d). CNR4 is Iran's last man-made reservoir in the series, receiving overflow from CNR1, 2 and 3 when these reservoirs are filled in April-May by spring flow. Thus, the area of CNR4 starts to increase after April-May. Based on the falling limb of the boxplots in Fig. 2e–g, the area of CNR1, 2 and 3 decreased in October, November and December because of conveying water to CNR4 (i.e., the rising limb of the boxplot shown in Fig. 2h). This operational strategy prepares CNR1, CNR2 and CNR3 to capture inflow in April-May by lowering the water level in CNR1 to maximize the discharge of the Feeder Canal (Fig. 1d), which is why the area of CNR4 is the highest during this period.

After April-May, the lakes gradually decreased to less than 5% of maximum area due to low inflow (falling limb of monthly inflow hydrograph in Fig. 5d) and high evaporation rate in the desert climate. Based on available images from Landsat and MODIS satellites from 1987 to 2020 (Fig. 2), between 1990 and 1999, all the Hamun Lakes had a large area. The highest inflow of Hirmand River to Iran since 1960 occurred in 1990 (Fig. 1e). After the onset of a severe drought period in 1999 (SDI $= -1.5$) and 2000 (SDI < -2), shown in Fig. 5a, the annual maximum area of Hamun-i Puzak, Hamun-i Saburi has not change considerably, but the duration of complete desiccation is longer recently compared to before the dry years in the beginning of 2000s (Fig. 2a and b). On the other hand, Hamun-i Hirmand almost dried up (lower maximum annual area and longer complete desiccation in Fig. 2c). Gaud-i Zirreh (depth: $\approx$10 m), which is more than 10 times deeper than the other lakes, is the only water body in this system that did not completely desiccate immediately after the severe drought of 1999–2000 and 2001–2002 (SDI close to -2).

Rate of desiccation of Hamun lakes

In the beginning of March 1999, Hamun-i Hirmand was 950 km^2, i.e. half of the maximum area based on available satellite images since 1987. Hamun-i Hirmand dried up over the next eight months when inflow to Hamun Lakes was zero (Fig. 3). The slope of the desiccation line was lower when the lake's area was between 950 and 700 km^2 compared with when the area ranged 700–0 km^2, which means the shrinkage process accelerates as the water body becomes smaller (Fig. 3). Seventeen months after the lake's inflow was completely halted (started in March 1999), Hamun-i Puzak and Hamun-i Saburi dried up completely. The rates of desiccation (i.e., slope of the lines in Fig. 3) for Hamun-i Puzak, Hamun-i

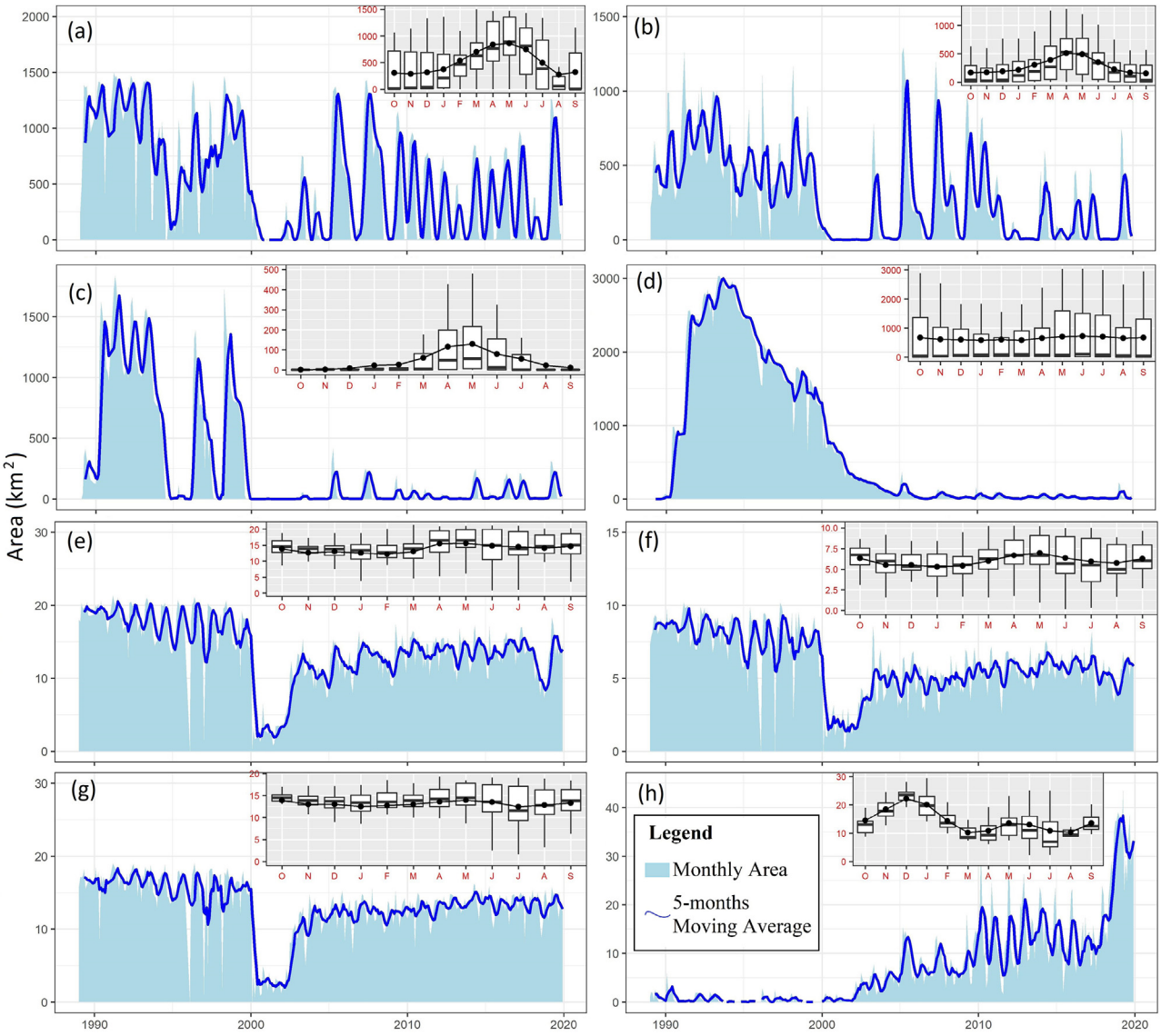

Fig. 2. Monthly area with box plot of area in each month for: a) Hamun-i Saburi, b) Hamun-i Puzak, c) Hamun-i Hirmand, d) Gaud-i Zirreh, e) CNR1, f) CNR2, g) CNR3 and h) CNR4.

Saburi, and Gaud-i Zirreh are steeper in the beginning. Gaud-i Zirreh is more resistant to inflow cut—Shile Canal inflow was zero after 1999—and its complete desiccation takes about 6 years (70 months) due to higher depth of this lake compared to the other lakes.

Water flow through Hamun lakes

We chose the 1988–1991 period to demonstrate how Hamun Lakes fill up and connect to each other (Fig. 4); since, in this period the lakes change from almost completely dry to full as captured by satellite images. The year 1988 ($SDI = 0.7$) was a transition year from the 1983–1987 dry period ($SDI < 0$ except 1985 when $SDI = 0.2$) to a very wet year in 1989 ($SDI = 1.1$) and an extremely wet year in 1990 ($SDI > 2$).

In the first months of 1988 (mildly wet based on Table 1), the Hamun Lakes were nearly empty due to the preceding drought period. The water area in the Northern Hamun Lakes started to increase in January to May by inflow in the same month but Gaud-i Zirreh kept shrinking because the level of water in northern Hamuns was not enough to feed the Shile Canal (compare Fig. 4, 1988-03 and 1988-05; also overflow between northern Hamuns is observable). All the Hamun Lakes shrank (Fig. 4, compare 1998–05 and 1988–07) during May-November 1988 due to reduced inflow in May (to almost zero) and water loss to evaporation. Inflow in December 1988 and January 1989 raised the water area in the northern lakes (Fig. 4, compare 1988–12 and 1989–02) immediately. A similar pattern is observed in 1989 (very wet year) when inflow was enough to reach Hamun-i Hirmand, although the Shile Canal and consequently Gaud-i Zirreh were not fed (Fig. 4, 1989-04). In 1990 (extremely wet year), inflow was the highest since 1960 and Shile Canal delivery increased the water area in Gaud-i Zirreh (Fig. 4, 1990-01). When inflow decreased in May 1990, the shallow lakes upstream of the Shile Canal, lost considerable area immediately. It took longer for deeper portions of the cascading lakes to desiccate in response to decreased inflow.

In March 1991 maximum recorded monthly inflow (4.5 km^3) of the Hirmand River entered Iran. Maximum area for Hamun-i Puzak (1,300 km^2) and Hamun-i Saburi (1,500 km^2) was observed in this month but the maximum area of Hamun-i Hirmand (1,800 km^2) occurred one month later (April 1991). The area of Hamun-i Hirmand in March 1991 was 1,700 km^2. The largest area for Gaud-i

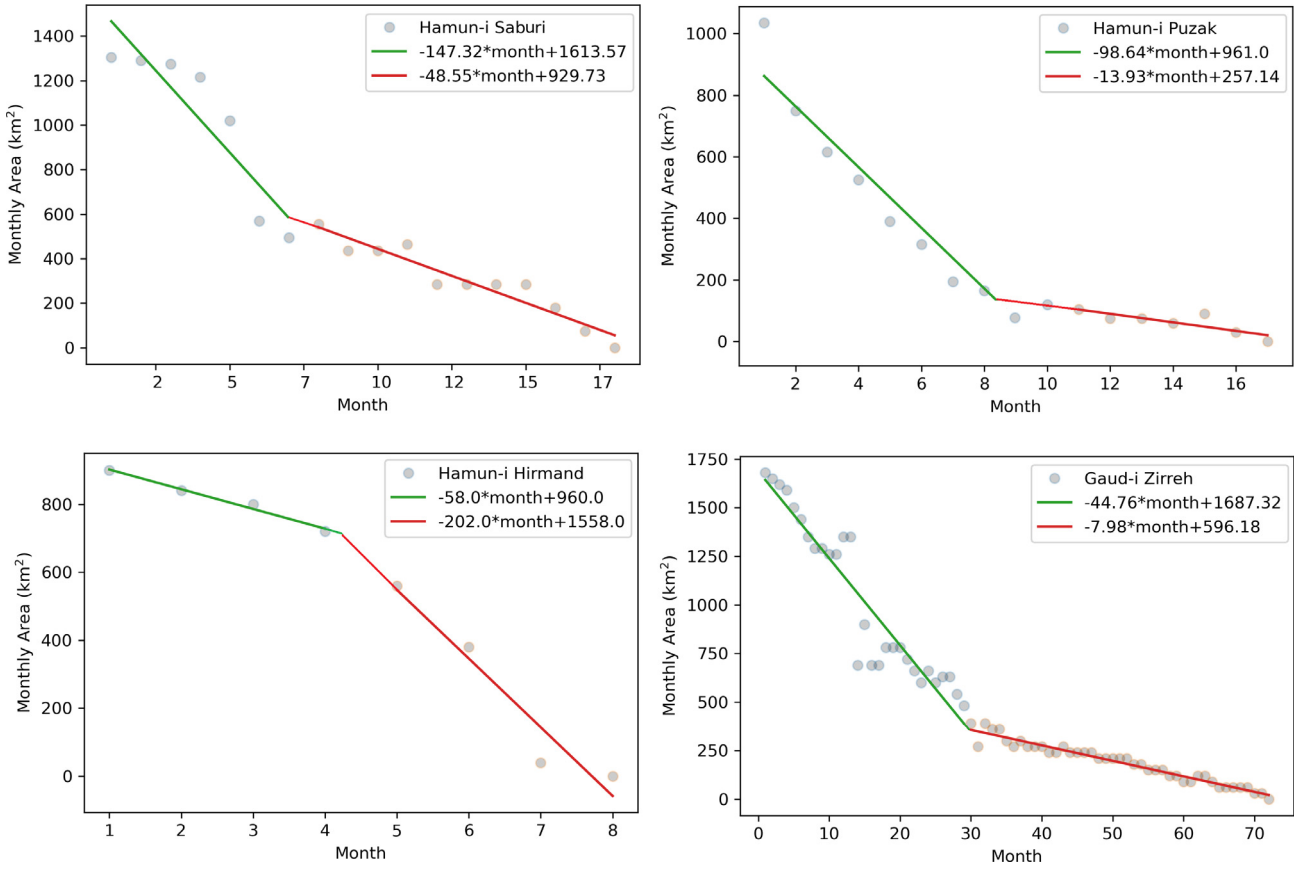

Fig. 3. Desiccation of Hamun Lakes rate based on number of months passing from March 1999 when inflow became zero to each of lake.

Zirreh in 1991 was 2,600 km^2 observed four months later in July. Therefore, the time lags for water conveyance from Hamun-i Puzak and Hamun-i Saburi to Hamun-i Hirmand and finally to Gaud-i Zirreh were almost one and four months, respectively. Additionally, the maximum area of Gaud-i Zirreh was 3,000 km^2, which occurred more than 25 months later (in June 1993) because of accumulating inflows in the preceding years.

Drought in the Hirmand River sub-basin

The large gap between SPI and SDI occurs after 2004. The correlation coefficients before and after this year are 0.70 and 0.13, respectively reveal a drastic change in the relationship between upstream precipitation and downstream (in the border) inflow. This gap between precipitation and inflow continues until the SPI-SDI correlation becomes negative (i.e., −0.63 after 2010). Before 1990, SDI values were almost always (except 1962 and 1984) larger than SPI (on average 0.65 larger) (Fig. 5a). However, after 1990, the SDI was lower than SPI (except 1994, 1998, 1999 and 2005). The average difference between SDI and SPI was −0.9, −1.6 and −2.2 after 1990, 2004 and 2010 respectively (Fig. 5a). Based on Table 1, these gaps between the two indices will considerably affect the dry or wet classification of the year. For example, in water year 2014–2015, SPI has the highest value indicating an extremely wet year in terms of upstream precipitation. However, in this year and based on inflow at the border, SDI is less than −1 which implies a moderately dry year.

The mean annual precipitation in the whole Hirmand sub-basin (Fig. 1a) has the highest correlation with the precipitation upstream of Kajaki Dam (≈ 0.97, ESM Fig. S4). The mean precipitation in the Hindu Kush mountainous region is higher than other parts of the basin (ESM Fig. S3b); however, the correlation between precipitation in mountainous parts of the basin and lower regions downstream of Kajaki Dam is low (≈ 40%). In other words, according to SPI, the wet and dry cycles in the Hirmand sub-basin are governed by precipitation amounts in the upper parts of the sub-basin rather than downstream of Kajaki Dam (ESM Appendix B). This means that wet conditions may be observed upstream of Kajaki Dam while downstream portions of Hirmand River may be characterized by dry condition based on precipitation. High climatic variation of the Helmand Basin is important because the runoff in the upstream wet snow climate (Ds) and warm temperate climate (Cs) is a major contributor to the area of Hamun Lakes in the lower desert climate (BW). Also, the monthly distribution of precipitation in the Helmand Basin shows that March is often the wettest month of the year (Fig. 5d) even though the highest inflow of the river at the border occurs more frequently with some time lag in April or May (more detail in ESM Appendix C).

Investigation of the lakes area in similar years in terms of inflow

After a long drought period between 1998 and 2004 (Fig. 5a), the Hamun Lakes changed from permanent waterbody to seasonal (Fig. 2a–d). Therefore, the lakes area in similar years in terms of inflow before and after the drought period has changed significantly (Fig. 6). Also, in year 2008, CNR4 is inaugurated. The capacity of this reservoir is more than 0.8 km^3, i.e. 40% of annual Hirmand River flow into Iran in the last 10 years. This reservoir has increased the water regulation capacity in the region by from 0.65 to 1.45 km^3, which can affect the area of the Hamun Lakes. In this regard, we compared the state of the lakes' area in similar

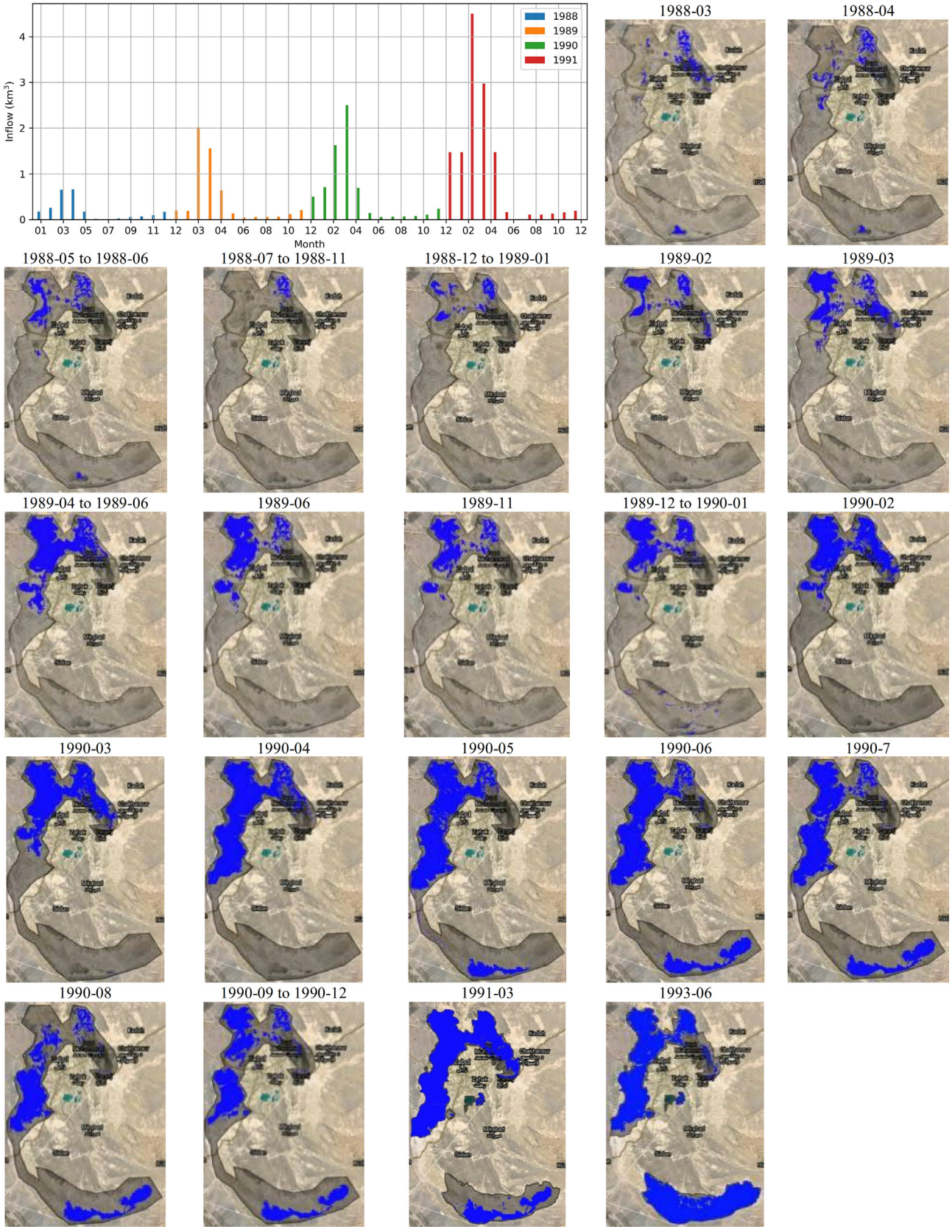

Fig. 4. Water transfer among the Hamun lakes (images are produced by Google Earth Engine Java Script API).

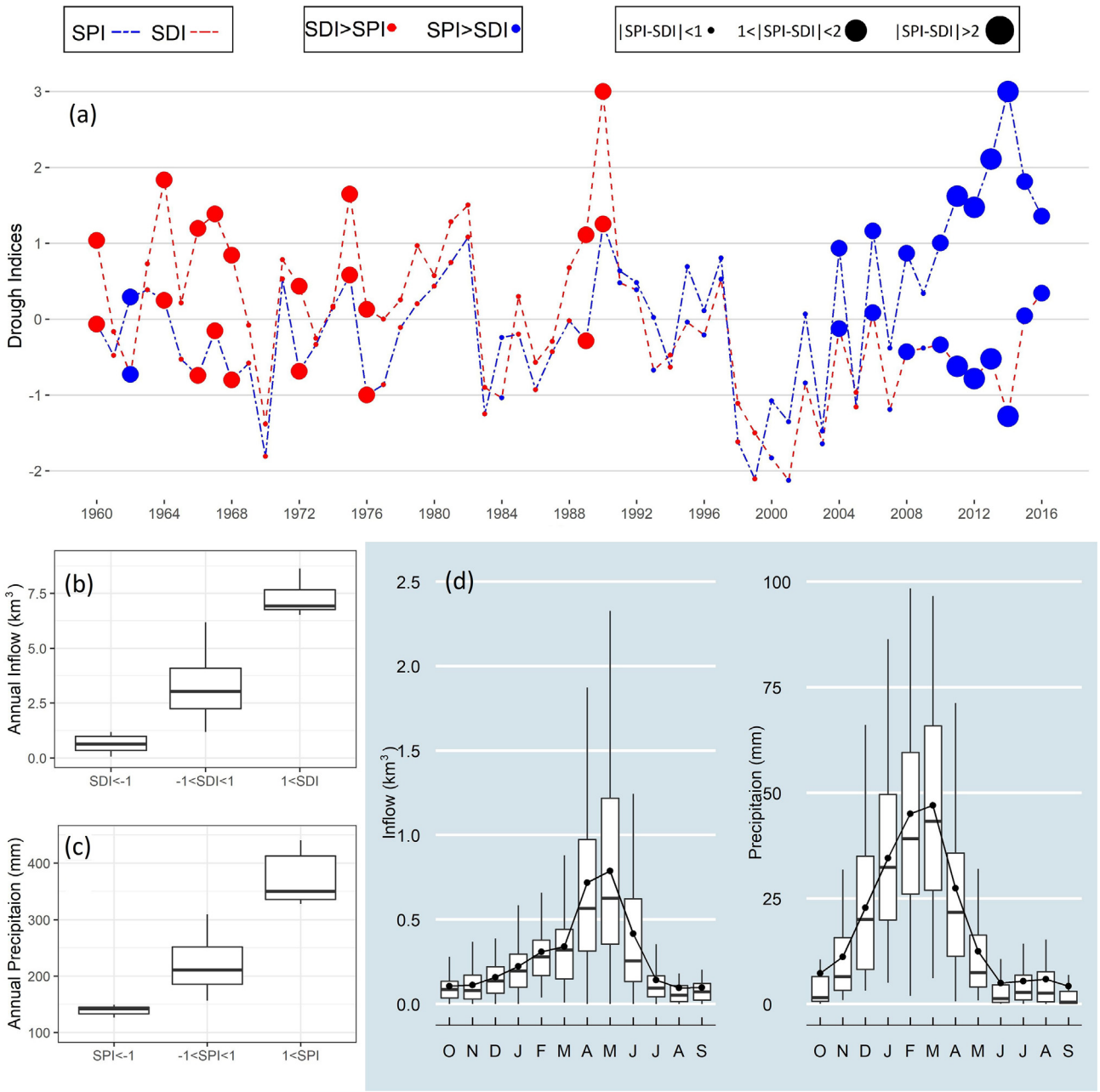

Fig. 5. a) SPI and SDI of Hirmand River sub-basin from 1960 to 2016 with difference of SPI and SDI in each year showing a shift in water management paradigm after 2003 when high precipitation does not correspond to high Hirmand River inflow in the location of border, b) annual precipitation based on different intervals of SPI c) annual inflow based on different intervals of SDI and d) the long-term monthly boxplots of Inflow and precipitation.

hydrological conditions in terms of Hirmand River deliveries to Iran before and after drought period, i.e., 1992/2016, 1996/2009 and 1993/2011 (Fig. 6 to c).

In 1992 (inflow ≈ 4 km^3), the area of Hamun-i Hirmand, Hamun-i Saburi and Hamun-i Puzak were 1,600, 1,500 and 1,000 km^2, respectively, which decreased by 55, 43 and 87% in a similar condition in 2016 (Fig. 6a). In 2009 (inflow ≈ 2.5 km^3) Hamun-i Hirmand lost 86% of its area compared to 1996 (Fig. 6b). The areal loss of this lake in 2011 (inflow ≈ 2 km^3) was 95% compared to 1993 (Fig. 6c). Likewise, the area of Hamun-i Puzak and Hamun-i Saburi decreased 57 and 45% in 2011 compared to similar conditions in 1993 (Fig. 6c). However, the gap between area of Hamun-i Saburi and Hamun-i Puzak in 1996 and 2009 decreases. In 2009, only 19 and 11% of these lake's areas, respectively, were lost compared to 1996 (Fig. 6b). There are no streamflow data available for other rivers that feed the Hamun Lakes, but water presence in a wetland in the northeast of Hamun-i Puzak (Fig. 6b) shows considerable inflow from Khash River and likely other rivers in the north (Fig. 1b). In 2009, more than 70% of this wetland was full (even more than its area in 1996). However, the wetland was dry in all other years after CNR4 operation (i.e., 2009 is an exceptional year).

The Hamun Lakes have changed from permanent to seasonal water bodies. Therefore, the initial area of the lakes is very important when comparing the effect of Iran's regulations between the international border and the lakes in similar years in terms of inflow. In 1986 and 2011, the recorded Hirmand River inflow by the border gauge is about 2 km^3 (Fig. 1e), and the monthly distribution of the flow is similar in both years (ESM Fig. S5c). Also, the area of northern Hamun Lakes (i.e., Saburi, Puzak and Hirmand)

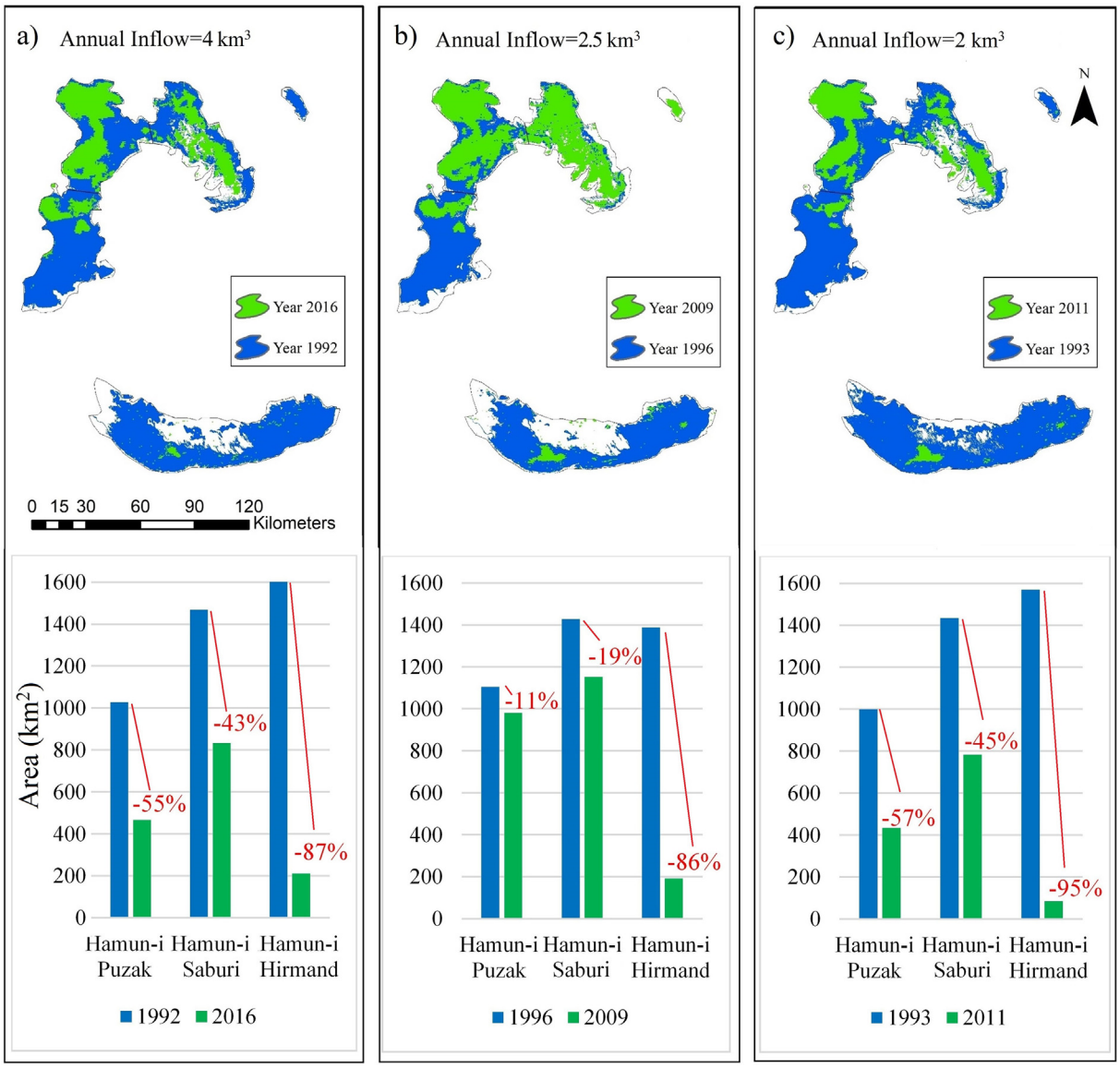

Fig. 6. Comparison between areas of the Hamun Lakes in similar years in terms of the Hirmand River annual inflow delivery in the border; percentage of area decline before and after long dry period (1998–2004) are shown in each bar plot.

in the beginning of these years is about 200 km^2. Therefore, the comparison between these two years can be a good indicator of recent anthropogenic changes between the border and the lakes on the Iranian side (e.g., agricultural development, CNR4 effect, etc.). In 1986, the area of northern Hamun Lakes increased to 2,300 km^2 in May. However, in 2011, the area reached 1,200 km^2 in the same month, a 48-percent decrease compared to 1986.

Monthly response of Hamun lakes area to Hirmand River flow

Monthly inflow can largely affect the area of Hamun-i Puzak and Hamun-i Saburi in the same month (Fig. 7a and b) because water retention time in connected Hamun Lakes above Shile Canal is small due to their low depth (shown in Figs. 3 and 4). When monthly Hirmand flow at the border is less than 0.5 km^3, the area of Hamun-i Puzak is most likely to be less than 500 km^2 (Fig. 7a). Also, when inflow increases from 0.5 to between 0.5 and 1 km^3, the area is more likely to exceed 500 km^2. Also, Hamun-i Saburi is expected to be larger than 500 km^2 when inflow in border rises from below 0.5 to above 0.5 km^3 (Fig. 7b). The area of this lake increases to more than 1250 km^2 when the Hirmand River delivery to Iran exceeds 1 km^3. Likewise, areas greater than 500 km^2 are expected for Hamun-i Hirmand when inflow increases (Fig. 7c). Boxplots of Hamun-i Hirmand and Gaud-i Zirreh have a considerable overlap (Fig. 7c and d) so there is no specific relation between Hirmand River inflow in border and their area in the same month. The areas of Hamun-i Hirmand and, especially Gaud-i Zirreh were very low after 2000 (Fig. 2c and d), indicating that Hirmand River inflow does not reach these lakes, and such comparison is not possible. Gaud-i Zirreh has higher water retention time which resulted in higher dependence of this lake's area to water accumulation in the preceding months.

Discussion

Hamun Lakes are responding to a shift in water management paradigm in a hydro politically complex transboundary basin where competition over limited water resources is rising. The

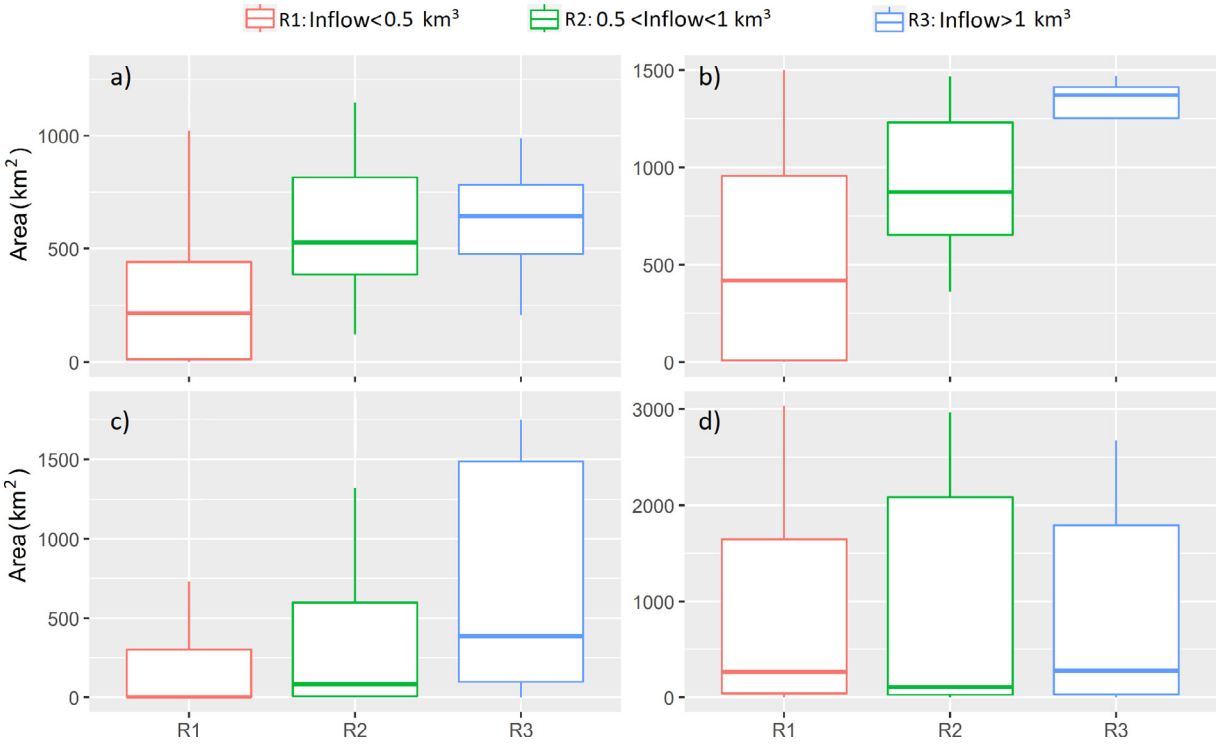

Fig. 7. Consequence of incrementally increasing Hirmand River monthly inflow by 0.5 km^3 on area of a) Hamun-i Puzak, b) Hamun-i Saburi, c) Hamun-i Hirmand, and d) Gaud-i Zirreh.

new paradigm is intensified after 2004 which has marginalized environmental flows to the lake as detected by large gap between SDI and SPI. The lakes are experiencing increased environmental flow stress mainly due to human modifications and flow regulation. The continuation of this trajectory is expected to amplify adverse environmental, socio-economic, and public health impacts associated with more frequent and prolonged desiccation of the lakes. It is urgent to recognize environmental water security as an important element of region's sustainability and plan practical steps to increase binational cooperation to prevent extensive socio-ecological impacts.

The high correlation between SPI and SDI from 1960 to 2003 shows that high precipitation naturally will lead to high runoff in the Hirmand River sub-basin. The large discrepancy between SPI and SDI after 2004 is a strong evidence about the effects of recent anthropogenic modifications on the Hamun Lakes. Water regulation upstream of the Hirmand River in Afghanistan has become more intensive, decreasing the deliveries to Iran as a new phenomenon in the basin. As an example, before 2010, the maximum recorded annual precipitation of the Hirmand River sub-basin was 330 mm in water year 1989–1990, which led to the maximum flow into Iran since 1960 (i.e., 12 km^3). While the annual precipitation water year 2014–2015 (473 mm) was 40% larger than the 1990 rainfall, the Hirmand River inflow in the border in this year was 30% of the flow delivered in 1990 (i.e., less than 4 km^3), indicating greater upstream regulation in Afghanistan. Reduction of the Hirmand River flow to Iran has been attributed by Afghanistan to a reduction in precipitation (Mianabadi et al., 2020). We show in this study that annual precipitation over the basin increased significantly after 2000 (Fig. 5a and ESM Fig. S2). Likewise, using remote sensing data for 34 years, Mianabadi et al. (2020) showed that the frequency and amount of heavy precipitation have been increasing over the mountainous areas which are the main source of the Hirmand River flow. Also, the total irrigated area in the Hirmand River sub-basin between the Kajaki Dam and the border has increased 62% from 1990 to 2011 (Hajihosseini et al., 2020), significantly increasing the upstream agricultural water demand.

Increased regulation of Hirmand River flow in this transboundary basin has weakened the hydrologic conditions to sustain the lakes. Based on the inflow of Hirmand to Iran, three major hydrological droughts occurred in the 1970s, 1980s and 2000s (Fig. 1e). These droughts prompted the Iranian government to sign a treaty with Afghanistan in 1973 to share Hirmand River flow, construct CNR1-3 in 1983, and CNR4 in 2008 to store water to meet regional demand, i.e., domestic and agricultural uses. The cumulative capacity of CNRs (≈1.5 km^3) plus 0.3 km^3 of annual evaporation from their surfaces amounts to about 95% of the annual average inflow of Hirmand River to Iran from 1995 to 2016 (≈1.9 km^3 shown in Fig. 1e). While CNRs have been effective in helping meet the water demand in the Sistan region, they have created a tradeoff by causing the area of the Hamun Lakes to decline. The large area of CNRs (Fig. 2e–h) in all years (except extremely dry years in 2000 and 2001), regardless of the SDI value, is an artifact of the priority given to filling the CNRs as much as possible to meet water demands in Iran. Once CNRs are full, the overflow is conveyed to Hamun Lakes. Low monthly areal variation of CNRs compared to Hamun Lakes denotes their importance for water supply, which is an impetus for more than doubling the capacity of the them in 2008 by adding CNR4. Quantifying the explicit effect of CNR4 on the lakes is complicated by the lack of flow data from all the tributaries as previously mentioned above. However, the surface areas of Hamun-i Puzak and Saburi are quite sensitive to monthly inflow variation of 0.5 km^3 (60% of CNR capacity). For example, the average area of Hamun Puzak and Saburi can be doubled if monthly flow of the Hirmand River increases from below 0.5 to between 0.5 and 1 km^3 (Fig. 7a and b). This illustrates the environmental water stress caused by diverting up to 0.81 km^3 to be stored in CNR4. The comparison between similar years in

terms of inflow and initial area of the lakes in January before and after CNR4 (i.e., 1986 and 2011) showed that the area of the northern Hamun Lakes (Puzak, Saburi and Hirmand) in 1986 was almost two times larger than the corresponding area in 2011. A study reported that, from 2010 to 2019, when all the anthropogenic pressures in the basin were in full effect, the average surface area of the Hamun Lakes could be 112% larger without water diversion by CNR4 (ModaresiRad et al., 2022).

The effects of increased water regulation propagate back into Afghanistan in the lower elevation downstream most sections of the basin. Gaud-i Zirreh, which is more resistant to desiccation than other lakes, nearly dried out after 2005 prior to the operation of CNR4. For example, although inflow in 1993 is less than 1992, Gaud-i Zirreh area is highest in 1993 ($\approx$3000 km^2) because of accumulated water from extremely wet (1990: inflow $\approx$ 12 km^3) and mildly wet (1991: inflow $\approx$ 5 km^3 and 1992: ,$\approx$ 4 km^3) years. Therefore, the desiccation of Gaud-i Zirreh should mainly be attributed to Hirmand River regulation in Afghanistan (annual inflow decreased from 4 to 1.9 km^3 shown in Fig. 1e) which is worsened by reservoir construction in Iran (CNR4) and Afghanistan (Kamal-Khan dam) next to border.

More than 1700 km^2 of cropland development is planned to be irrigated by the Kamal-Khan Dam in the future (Mianabadi et al., 2021). Therefore, the agricultural water needs will further increase on the Afghanistan side over time. Eight reservoirs in the basin (Fig. 1a) with a collective water storage capacity of more than 4.5 km^3 (share of Afghanistan 67%) regulate flow intensively. The lakes are desiccating despite the fact that the Hirmand River inflow at the international border has averaged 1.9 km^3 (1995–2016), twice the designated flow in the 1973 treaty. This indicates that the designated amount of water delivery in the treaty from Afghanistan and frequency and timing of deliveries do not suffice to meet both human water demands on the Iranian side while providing environmental flows to the lakes. The inauguration of Kamal-Khan dam in March 2021 adds another control on the magnitude and timing of flow deliveries to Iran, which could increase downstream stress and aggravate the condition of the lakes. It is time to clarify the environmental dimensions of the 1973 treaty in light of changing water supply and demand conditions on both sides of the border.

The 1999–2004 drought was the most severe on record going back to 1830 (Williams-Sether, 2008). After this dry period, the frequency and severity of dust storms has significantly increased (Rashki et al., 2012). This affects the livelihood of more than 1.1 million people who rely on Hirmand River inflow and Hamun Lakes in the Sistan region (Rashki et al., 2013). More than 25% of the population migrated from Sistan region due to environmental and economic situation after Hamun Lakes desiccation (ICANA, 2015). In 1977 more than 55% of Sistan inhabitants in Iran worked in the agricultural sector but this ratio has reduced to less than 22% in 2015 due to water scarcity and droughts (Ministry of Cooperatives Labour and Social Welfare Iran, 2017). Drought has negatively impacted fisheries which have been brought to a halt (Rashki et al., 2012) and caused high unemployment (Iranian Consultative Assembly News Aagency (ICANA) (2012)). The unemployment and declining quality of life can undermine border security due to potential links to unlawful economic activities, and in some cases terrorism (Bagchi and Paul, 2018). The desiccation of the Hamun Lakes has hydro-political, ecological, climatic, socio-economic, and legal complexities that go far beyond a hydrological assessment. Nonetheless, the results of this investigation shed light on the hydroclimatic aspects of this vulnerable socio-ecological system, calling for action and further interdisciplinary research to understand the root causes and potential consequences of the desiccation of the Hamun Lakes to inform mitigation efforts.

Conclusions

Hamun Lakes are consist of three connected Lakes (Hamun-i Puzak, Hamun-i Saburi and Hamun-i Hirmand) above Shile Canal and a deeper terminal lake (Gaud-i Zirreh). The first three cascading lakes are very shallow, and they respond rapidly to monthly Hirmand River inflow variation. A shift in upstream regulations of the Hirmand River in Afghanistan has changed post-2004 water deliveries at the international border. From 1960 to 2003, Standardized Discharge Index (SDI) and Standardized Precipitation Index (SPI) were highly correlated (70%), meaning high river flow was expected to feed the lakes due to high precipitation over the Hirmand River sub-basin. However, the correlation changed to 0.13 in the periods 2004–2016 indicating a drastic decline in the Hirmand River flow downstream despite large amounts of upstream precipitation over its sub-basin. This gap kept increasing and SPI-SDI correlation became negative (≈ -0.63) between 2010 and 2016. Upstream regulations are the main cause of inflow delivery reduction to the lakes. The construction of Chah Nimeh Reservoir 4 (capacity of 0.81 km^3 for domestic and agricultural use in a socio-economically disadvantaged region of Iran) and Kamal-Khan Dam (capacity 0.05 km^3) has aggravated the situation. The decline of the socio-ecological system due to unsustainable water management in this transboundary region is expected to have detrimental impacts on the condition of the residents (e.g., dust storms). Therefore, revisiting the 1973 treaty between riparian countries to share the Hirmand River inflow considering the environmental right of the lakes is recommended to improve the condition of the region.

CRediT authorship contribution statement

Mahdi Akbari: Conceptualization, Methodology, Software, Data curation, Writing – original draft, Validation, Visualization, Investigation, Writing – review & editing. **Ali Mirchi:** Conceptualization, Validation, Writing – original draft, Supervision. **Amin Roozbahani:** Conceptualization, Data curation, Validation, Investigation. **Abror Gafurov:** Supervision. **Bjørn Kløve:** Conceptualization, Writing – original draft, Supervision. **Ali Torabi Haghighi:** Conceptualization, Methodology, Writing – original draft, Validation, Investigation, Writing – review & editing, Supervision.

Declaration of Competing Interest

The authors declare that they have no known competing financial interests or personal relationships that could have appeared to influence the work reported in this paper.

Acknowledgements

The authors are thankful to Dr. Kaveh Madani for his valuable comments. The second author acknowledges the Iranian and Persian Gulf Studies professorship from Oklahoma State University's School of Global Studies and Partnerships.

Funding

This work was supported by the University of Oulu Graduate School (UniOGS).

Electronic Supplementary Material

Electronic Supplementary Material of this article can be found online at https://doi.org/10.1016/j.jglr.2022.05.004.

References

Absaran Consulting Company, 2015. Chah Nimeha water resources planning report, studies of the second phase of water supply in Sistan plain (in Farsi).

Afganistan Ministry of Urban Development Affairs, 2015. The State of Afghan Cities Report 2015.

AghaKouchak, A., Norouzi, H., Madani, K., Mirchi, A., Azarderakhsh, M., Nazemi, A., Nasrollahi, N., Farahmand, A., Mehran, A., Hasanzadeh, E., 2015. Aral Sea syndrome desiccates Lake Urmia: call for action. J. Great Lakes Res. 41 (1), 307–311.

Ahlers, R., Brandimarte, L., Kleemans, I., Sadat, S.H., 2014. Ambitious development on fragile foundations: Criticalities of current large dam construction in Afghanistan. Geoforum 54, 49–58. https://doi.org/10.1016/j.geoforum.2014.03.004.

Akbari, M., Baubekova, A., Roozbahani, A., Gafurov, A., Shiklomanov, A., Rasouli, K., Ivkina, N., Kløve, B., Haghighi, A.T., 2020. Vulnerability of the Caspian Sea shoreline to changes in hydrology and climate. Environ. Res. Lett. 15 (11), 115002. https://doi.org/10.1088/1748-9326/abaad8.

Akbari, M., Torabi Haghighi, A., Aghayi, M.M., Javadian, M., Tajrishy, M., Kløve, B., 2019. Assimilation of satellite-based data for hydrological mapping of precipitation and direct runoff coefficient for the Lake Urmia Basin in Iran. Water 11, 1624. https://doi.org/10.3390/w11081624.

Alam, K., Trautmann, T., Blaschke, T., 2011. Aerosol optical properties and radiative forcing over mega-city Karachi. Atmos. Res. 101 (3), 773–782.

Alborzi, A., Mirchi, A., Moftakhari, H., Mallakpour, I., Alian, S., Nazemi, A., Hassanzadeh, E., Mazdiyasni, O., Ashraf, S., Madani, K., Norouzi, H., Azarderakhsh, M., Mehran, A., Sadegh, M., Castelletti, A., AghaKouchak, A., 2018. Climate-informed environmental inflows to revive a drying lake facing meteorological and anthropogenic droughts. Environ. Res. Lett. 13 (8), 084010.

Amini, A., Ghoreishi, S.Z., Mianabadi, H., 2021. Understanding 1973 the Helmand Treaty by Invoking Rules of Interpretation According to Vienna Convention 1969. Dep. Water Irrig. Available online https//jwim. ut. ac. ir/article_82737. html (accessed 23 August 2021).

Ashouri, H., Hsu, K.-L., Sorooshian, S., Braithwaite, D.K., Knapp, K.R., Cecil, L.D., Nelson, B.R., Prat, O.P., 2015. PERSIANN-CDR: Daily Precipitation Climate Data Record from Multisatellite Observations for Hydrological and Climate Studies. Bull. Am. Meteorol. Soc. 96, 69–83. https://doi.org/10.1175/BAMS-D-13-00068.1.

Bagchi, A., Paul, J.A., 2018. Youth unemployment and terrorism in the MENAP (Middle East, North Africa, Afghanistan, and Pakistan) region. Socioecon. Plann. Sci. 64, 9–20. https://doi.org/10.1016/j.seps.2017.12.003.

Boschetti, M., Nutini, F., Manfron, G., Brivio, P.A., Nelson, A., Schumann, G.-P., 2014. Comparative analysis of normalised difference spectral indices derived from MODIS for detecting surface water in flooded rice cropping systems. PLoS One 9 (2).

Chaudhari, S., Felfelani, F., Shin, S., Pokhrel, Y., 2018. Climate and anthropogenic contributions to the desiccation of the second largest saline lake in the twentieth century. J. Hydrol. 560, 342–353. https://doi.org/10.1016/j.jhydrol.2018.03.034.

Chen, J.L., Wilson, C.R., Tapley, B.D., Save, H., Cretaux, J.F., 2017. Long-term and seasonal Caspian Sea level change from satellite gravity and altimeter measurements. J. Geophys. Res. Solid Earth 122, 2274–2290. https://doi.org/10.1002/2016JB013595.

Chipman, J.W., Lillesand, T.M., 2007. Satellite-based assessment of the dynamics of new lakes in southern Egypt. Int. J. Remote Sens. 28, 4365–4379. https://doi.org/10.1080/01431160701241787.

Dehgan, A., Palmer-Moloney, L.J., Mirzaee, M., 2014. Water security and scarcity: Potential destabilization in western Afghanistan and Iranian Sistan and Baluchestan due to transboundary water conflicts. Water and post-conflict peacebuilding 305.

Ehsani, M.R., Arevalo, J., Risanto, C.B., Javadian, M., Devine, C.J., Arabzadeh, A., Venegas-quiñones, H.L., Paige, A., Oro, D., Behrangi, A., 2020. Hydroclimatological and Vegetation Variabilities 1–18.

Farahmand, A., AghaKouchak, A., 2015. A generalized framework for deriving nonparametric standardized drought indicators. Adv. Water Resour. 76, 140–145.

Ghajarnia, N., Akbari, M., Saemian, P., Ehsani, M.R., Hosseini-Moghari, S.-M., Azizian, A., Kalantari, Z., Behrangi, A., Tourian, M.J., Klöve, B., others, 2021. Evaluating the Evolution of ECMWF Precipitation Products Using Observational Data for Iran: From ERA40 to ERA5.

Gorelick, N., Hancher, M., Dixon, M., Ilyushchenko, S., Thau, D., Moore, R., 2017. Google Earth Engine: Planetary-scale geospatial analysis for everyone. Remote Sensing of Environment 202, 18–27.

Goudie, A.S., Middleton, N.J., 2006. Desert dust in the global system. Springer Science & Business Media.

Goudie, A.S., Middleton, N.J., 2000. Dust storms in south west Asia. Acta Univ, Carolinae, Suppl, p. 7383.

Haghighi, A.T., Kløve, B., 2015. A sensitivity analysis of lake water level response to changes in climate and river regimes. Limnologica 51, 118–130.

Torabi Haghighi, A., Abou Zaki, N., Rossi, P.M., Noori, R., Hekmatzadeh, A.A., Saremi, H., Kløve, B., 2020. Unsustainability syndrome-from meteorological to agricultural drought in arid and semi-arid regions. Water (Switzerland) 12 (3), 838.

Hajihosseini, M., Hajihosseini, H., Morid, S., Delavar, M., Booij, M.J., 2020. Impacts of land use changes and climate variability on transboundary Hirmand River using SWAT. J. Water Clim. Chang. 11, 1695–1711.

Hamoon International Wetland Research Institute of Zabol University (HIWRI), 2017. Investigation of water requirement for Hamoon International Wetland in different water scenarios.

Hao, Z., AghaKouchak, A., Nakhjiri, N., Farahmand, A., 2014. Global integrated drought monitoring and prediction system. Sci. data 1, 1–10.

Helmand Commission, 1973. The 1973 Helmand River Treaty [WWW Document]. URL https://www.internationalwaterlaw.org/documents/regionaldocs/1973_Helmand_River_Water_Treaty-Afghanistan-Iran.pdf.

Hossenzadeh, S.R., 1997. One hundred and twenty days winds of Sistan. Iran Iran. J Res Geogr. 46, 103–127.

Huffman, G., Adler, R., Bolvin, D., Gu, G., Nelkin, E., Bowman, K., Hong, Y., Stocker, E., Wolff, D., 2007. The TRMM multi-satellite precipitation analysis: Quasi-global, multi-year, combined sensor precipitation estimates at fine scales. J. Hydrometeorol. 8, 28–55.

ICANA, 2015. 25% migration of Sistan people due to drought [WWW Document]. URL khabaronline.ir/news/587938 (accessed 8.25.20).

Iran Department of Environment (DOE), 2014. Determining the environmental flow needs of Hamun wetlands.

Iran Ministry of Enegry (MoE), 2013. Update of Sistan River studies (hydrological report).

Iranian Consultative Assembly News Aagency (ICANA), 2012. “Hamoon” is the artery of Sistan [WWW Document] accessed 8.25.20 https://www.icana.ir/Fa/News/248571/%22هامون%22شاهرگ-سیستان-است, .

Irannezhad, M., Torabi Haghighi, A., Chen, D., Kløve, B., 2015. Variability in dryness and wetness in central Finland and the role of teleconnection patterns. Theor. Appl. Climatol. 122 (3-4), 471–486.

Khazaei, B., Khatami, S., Alemohammad, S.H., Rashidi, L., Wu, C., Madani, K., Kalantari, Z., Destouni, G., Aghakouchak, A., 2019. Climatic or regionally induced by humans? Tracing hydro-climatic and land-use changes to better understand the Lake Urmia tragedy. J. Hydrol. 569, 203–217.

Kottek, M., Grieser, J., Beck, C., Rudolf, B., Rubel, F., 2006. World map of the Köppen-Geiger climate classification updated. Meteorol. Zeitschrift 15 (3), 259–263.

Lehner, B., Liermann, C.R., Revenga, C., Vörösmarty, C., Fekete, B., Crouzet, P., Döll, P., Endejan, M., Frenken, K., Magome, J., Nilsson, C., Robertson, J.C., Rödel, R., Sindorf, N., Wisser, D., 2011. High-resolution mapping of the world's reservoirs and dams for sustainable river-flow management. Front. Ecol. Environ. 9 (9), 494–502.

McKee, T.B., 1995. Drought monitoring with multiple time scales, in: Proceedings of 9th Conference on Applied Climatology, Boston, 1995.

Meteorological Department of Sistan and Baluchestan, 2020. 120-day wind speed [WWW Document]. URL https://sbmet.ir/(accessed 6.3.21).

Mianabadi, A., Davary, K., Mianabadi, H., Karimi, P., 2020. International Environmental Conflict Management in Transboundary River Basins. Water Resour. Manag. 34, 3445–3464. https://doi.org/10.1007/s11269-020-02576-7.

Mianabadi, H., Alioghli, S., Morid, S., 2021. Quantitative evaluation of ‘ No-harm ’ rule in international transboundary water law in the Helmand River basin. J. Hydrol. 599,. https://doi.org/10.1016/j.jhydrol.2021.126368 126368.

Micklin, P.P., 1988. Desiccation of the Aral Sea: a water management disaster in the Soviet Union. Science (80-. 241 (4870), 1170–1176.

Milly, P.C.D., Dunne, K.A., 2016. Potential evapotranspiration and continental drying. Nat. Clim. Chang. 6, 946–949.

Ministry of Cooperatives Labour and Social Welfare Iran, 2017. Employment status of Sistan and Baluchestan province.

Ministry of Energy (MoE), 2015. Report on water resources and consumption of Sistan and Baluchestan province.

Ministry of Energy (MoE) Studies of the second phase of water supply in Sistan plain 2014 Tehran.

Miri, A., Ahmadi, H., Ghanbari, A., Moghaddamnia, A., 2007. Dust storms impacts on air pollution and public health under hot and dry climate. Int J Energy Env. 2, 101–105.

ModaresiRad, A., Kreitler, J., Abatzoglou, J.T., Fallon, K., Roche, K., Sadegh, M., 2022. Anthropogenic stressors compound climate impacts on inland lake dynamics: The case of Hamun Lakes. Sci, Total Environ, p. 154419.

Ouma, Y.O., Tateishi, R., 2006. A water index for rapid mapping of shoreline changes of five East African Rift Valley lakes: an empirical analysis using Landsat TM and ETM+ data. Int. J. Remote Sens. 27, 3153–3181. https://doi.org/10.1080/01431160500309934.

Pekel, J.F., Cottam, A., Gorelick, N., Belward, A.S., 2016. High-resolution mapping of global surface water and its long-term changes. Nature 540, 418–422. https://doi.org/10.1038/nature20584.

Rahimi, R., Tavakol-Davani, H., Graves, C., Gomez, A., Valipour, M.F., 2020. Compound inundation impacts of coastal climate change: Sea-level rise, groundwater rise, and coastal precipitation. Water (Switzerland) 12, 1–16. https://doi.org/10.3390/w12102776.

Rashki, A., Kaskaoutis, D.G., Goudie, A.S., Kahn, R.A., 2013. Dryness of ephemeral lakes and consequences for dust activity: The case of the Hamoun drainage basin. Southeastern Iran. Sci. Total Environ. 463–464, 552–564. https://doi.org/10.1016/j.scitotenv.2013.06.045.

Rashki, A., Kaskaoutis, D.G., Rautenbach, C.J.deW., Eriksson, P.G., Qiang, M., Gupta, P., 2012. Dust storms and their horizontal dust loading in the Sistan region. Iran. Aeolian Res. 5, 51–62.

K. Rokni A. Ahmad A. Selamat S. Hazini Water Feature Extraction and Change Detection Using Multitemporal Landsat Imagery Remote Sensing 6 5 4173 4189.

Rouse Jr, J.W., 1973. Monitoring the vernal advancement and retrogradation (green wave effect) of natural vegetation. https://ntrs.nasa.gov/api/citations/19730017588/downloads/19730017588.pdf.

Saemian, P., Hosseini-Moghari, S.-M., Fatehi, I., Shoarinezhad, V., Modiri, E., Tourian, M.J., Tang, Q., Nowak, W., Bárdossy, A., Sneeuw, N., 2021. Comprehensive evaluation of precipitation datasets over Iran. J. Hydrol. 603,. https://doi.org/10.1016/j.jhydrol.2021.127054 127054.

Schneider, U., Becker, A., Finger, P., Meyer-Christoffer, A., Rudolf, B., Ziese, M., 2011. Monthly land-surface precipitation from rain-gauges built on GTS-based and historic data. Glob. Precip. Clim. Cent.(GPCC), Dtsch. Wetterdienst, doi 10.

Shukla, S., Wood, A.W., 2008. Use of a standardized runoff index for characterizing hydrologic drought. Geophys. Res, Lett, p. 35.

Statistical Center of Iran, 2016. Results of the general population and housing census in 2016 [WWW Document] accessed 11.26.20 https://www.amar.org.ir/english, .

Tadono, T., Nagai, H., Ishida, H., Oda, F., Naito, S., Minakawa, K., Iwamoto, H., 2016. Generation of the 30 M-mesh global digital surface model by ALOS PRISM. Int. Arch. Photogramm. Remote Sens. Spat. Inf, Sci, p. 41.

The Convention on Wetlands, 1975. Ramsar Sites Information Service [WWW Document]. URL https://rsis.ramsar.org/(accessed 1.1.20).

Thom, H.C.S., 1966. Some methods of climatological analysis. WMO Tech. Note81.

Thomas, V., Varzi, M.M., 2015. A legal licence for an ecological disaster: the inadequacies of the 1973 Helmand/Hirmand water treaty for sustainable transboundary water resources development. Int. J. Water Resour. Dev. 31 (4), 499–518.

WHO, 2016. Global Health Observatory data repository [WWW Document]. World Heal, Organ. https://apps.who.int/gho/data/view.main.AMBIENTCITY2016?lang=en (accessed 11.8.20.

Williams-Sether, T., 2008. Streamflow characteristics of streams in the Helmand Basin. Afghanistan, US Department of the Interior, US Geological Survey.

Abou Zaki, N., Torabi Haghighi, A., Rossi, P.M., Tourian, M.J., Bakhshaee, A., Kløve, B., 2020. Evaluating impacts of irrigation and drought on river, groundwater and a terminal Wetland in the Zayanderud Basin. Iran. Water (Switzerland) 12 (5), 1302.

Abou Zaki, N., Torabi Haghighi, A., Rossi, P., Xenarios, S., Kløve, B., 2018. An index-based approach to assess thewater availability for irrigated agriculture in sub-Saharan Africa. Water (Switzerland) 10 (7), 896.